Breakthrough Studies of Co_3O_4 Supported Activated Carbon Monolith for Simultaneous SO_2/NO_x Removal from Flue Gas

S. Kiman[a*], W.A. Wan Ab Karim Ghani[b], T.S.Y. Choong[c] and R. Umer[d]
Department of Chemical and Environmental Engineering, Faculty of Engineering, Universiti Putra Malaysia, 43400 Serdang, Selangor, Malaysia[a,b,c]
Institute of Technology Maju (ITMA), 43400 Serdang, Selangor, Malaysia[d]
+603-89466287, wanazlina@upm.edu.my[b].
+603-89466293, csthomas@upm.edu.my[c],
+601-34507820, umer.rashid@upm.edu.my[d],
* Corresponding author: +60108476412, gs48827@student.upm.edu.my[a]

Nomenclature

ACM	activated carbon monolith
Ce	equilibrium concentration of adsorbate (mg/L)
C_{inf}	initial concentration of adsorbate (mg/L)
C_{eff}	final concentration of adsorbate (mg/L)
DP	deposition precipitation method
HM	hydrothermal method
IM	impregnation method
hr	hours
	Langmuir isotherm equilibrium bonding energy of sorption in (L/g)
K_f	Freundlich isotherm adsorption capacity constant (L/g)
M	mass of sorbent (g)
MO	metal oxide
min	minutes
n	Freundlich adsorption intensity constant
	equilibrium adsorption capacity (mg/g)
	maximum adsorption capacity to form a complete monolayer on the surface (mg/g)
r^2	correlation coefficient
R_L	Langmuir separation factor (dimensionless)
t_b	breakthrough time
t_{sat}	saturation time

Graphical abstract

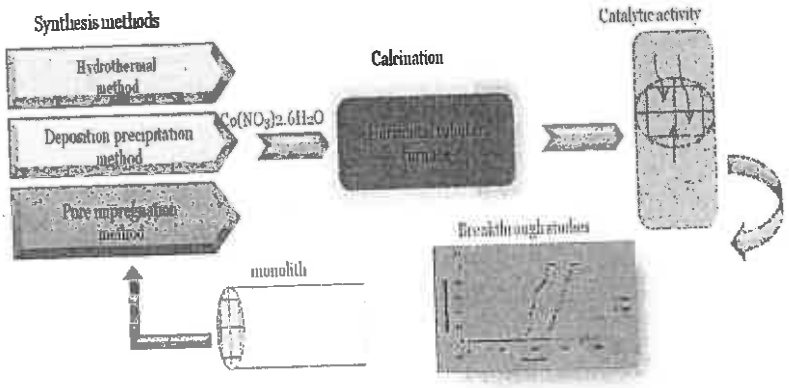

Abstract
This work investigates the deposition precipitation, pore volume impregnation and hydrothermal methods in the synthesis of activated carbon monolith with metal oxide (Co_3O_4). The catalyst activity was carried out for the simultaneous SO_2/NO_x removal from flue gas generated by burning coal to simulate the real life event occurring in power plant and other industries. The performance of the adsorbents in terms of synthetic method was found to be in the following order: HM-Co_3O_4/adsorbent>IM-Co_3O_4/adsorbent >DP-Co_3O_4/adsorbent. The Co_3O_4/adsorbent has a high affinity to NO_x adsorption and this influence is associated with the physical and chemical properties of the adsorbent and the operation conditions which were expressed through the plot of the breakthrough curve. The adsorption capacity, breakthrough and saturation times for SO_2 were found to be 123.1 mg/g, 86 min and 126 min while 130.2 mg/g, 124 min and 160 min were obtained for NO_x with respect to the best performed adsorbent. FTIR data provides the confirmation of SO_4^{2-} and NO_3^- ions accumulation on the adsorbent in the ranges of 700-450 cm^{-1}. Langmuir adsorption model, which is based on constant adsorption energy independence of surface coverage, fitted the experimental results.

Keywords: activated carbon monolith; breakthrough curves; sulfur dioxide and nitric oxide; synthesis

Highlight

- Three methods of synthesis were used to develop adsorbents
- First study to synthesized monolith and test in the laboratory with generated flue gas
- First study to demonstrate high NO_x adsorption capacity
- Langmuir and Freundlich were used to correlate the experimental data

1. Introduction

Environmental problems including haze, greenhouse effects and acid rain are caused by emission of gases such as sulfur dioxide (SO_2) and nitric oxide with its group of compounds (NO_x) where, NO in power plant flue gases was revealed to represents over 90 to 95% of total NO_x, other compounds are NO_2, NO_3, N_2O, N_2O_3, N_2O_4 and N_2O_5 [1-3], therefore, the requirements of emission standard for pollutants in power plants and other industries is recently rigorous. The mainstream gases abatement technique is mostly performed for single gas composition treatment [1] and the widely used emission control technologies are; wet flue gas desulfurization (WFGD) technology for the SO_2 removal and the selective catalytic reduction (SCR) or the selective non-catalytic reduction (SNCR) for NO_x removal. The ammonia-based WFGD compared with various WFGD processes has higher desulfurization efficiency, lower investment, useful byproducts and without secondary pollution but the technology is immature in large scale because of ammonia escape concern and aerosol phenomena [1,4]. The SCR is associated with poor catalyst durability (coverage of the catalyst by very fine dust particles,) and eventually to ammonia slip, with low NO_x reduction and high temperature requirement [4,5].

Adsorption is a simple and cost effective dry process method for removing process gases and vapors from air in a dry process [6]. Comparatively, dry process is preferred over wet process in terms of cost and environmental considerations, where wastewater and reheating energy requirement with a report of low pollutant removal are associated with the wet process [7]. Adsorption has the advantage of minimum secondary pollution production, low operational cost and applicable at lower pollutant concentrations [8]. According to Browski [9], solid adsorbents are utilize for dry adsorption, example are; activated carbon fibres and carbon molecular sieves, fullerenes and heterofullerenes, microporous glasses and nanoporous, carbonaceous and inorganic materials, this is due to their catalytic, magnetic, optical and thermal properties. Activated carbon has large surface area, but its breakthrough capacity becomes low as temperature increases [10] moreover, Wang et al. [11] relates granular carbon catalysts with high flow resistance and plugging problems through fly ash present in flue gas thereby limiting their commercial application. The use of monolith in separation and purification applications is advantageous over granules, in their work, Hosseini, et al. [12] found that a piece permeable mass of monolith can separate species better than a cluster of packed particles.

There is a sense in which monolith is used as adsorbent having the following advantages; high void fraction, uniform flow distribution, large geometric surface area, resistance to thermal shock, low pressure drop at high flow rate and high dust tolerance [13], several literatures discussed monolith in detail [14,15,16,17] Most of the researches conducted pertaining flue gases used simulated flue gas in place of the flue gas in the laboratory for catalyst test, few studies are mentioned [18]. Challenges faced by emission control integration technologies

mentioned earlier can be address by the simultaneous removal of SO_2 and NO_x using high efficient, low cost and environmental friendly catalyst with high activity at low temperature.
There is no reported work that solemnly discusses the Co_3O_4 supported monolith impregnation for the purpose of simultaneous removal of SO_2/NO_x with laboratory generated flue gas. Since the catalyst activity is strongly influenced by the preparation technique of the MO, therefore, in this work we carried out three different synthetic methods (hydrothermal, deposition precipitation, pore volume impregnation) to impregnate activated carbon monolith with Co_3O_4. The breakthrough curve studies were carried out and adsorption models based on Langmuir and Freundlich models for the description of simultaneous adsorption of SO_2 and NO_x over Co_3O_4/ACM adsorbent were performed.

2. Materials and methods

2.1. Adsorbent

The ceramic monoliths were purchased from Beihai Huihuang Chemical Packing Co. Ltd., China. Table1 presents the specifications of monolith structure used.

Table 1
Specifications of bare monolith

Monolith	Cells	Chemical compositions
cross section circular	channel square	SiO_2 50.9 ± 1.0%
surface area 1cm^2/g	wall thickness 0.25 ± 0.02 mm	Al_2O_3 35.2 ± 1.0%
length 2.50 ± 0.02 mm	width 1.02 ± 0.02 mm	MgO 13.9 ± 0.5%
diameter 2.50 ± 0.02 mm	cells 400 (cpsi)	others <1%

2.2. Chemicals

Nitric acid (HNO_3, 65%), urea (CH_4N_2O) and cobolt nitrate hexahydrates ($Co(NO_3)_2.6H_2O$) were purchased from Sigma-Aldrich, Malaysia. All the chemicals and reagents used were of analytical reagent (AR) grade.

2.3. Monolith chemical pretreatment and activation

The monolith was oxidised by complete immersion in HNO_3 for 24 hr, followed by filtration and washing with deionised water severally then dried in an oven at 70 °C for 24 hr. Finally, the oxidized monolith was activated by heating in vertical furnace at heating rate of 5 °C min^{-1} to 850 °C for 4 hr with continues passage of nitrogen gas and cooled under the inert condition.

2.4. Catalyst Preparation

2.4.1. Pore volume wetness impregnation method

The activated carbon monolith (ACM) was impregnated with appropriate aqueous solution containing single cobolt nitrate hexahydrates ($Co(NO_3)_2.6.H_2O$) precursor. The mixture was heated with constant stirring at 70 °C and 300 rpm until the entire liquid evaporated then dried at 110 °C in an oven for 24 hr followed by heat treatment under nitrogen flow at a heating rate of 3 °C min^{-1} up to 500 °C for 4 hr.

2.4.2. Deposition precipitation method

A closed 350 mL reactor vessel equipped with pH meter, thermometer, and magnetic stirrer was loaded with 250 mL deionized water, ACM support and $Co(NO_3)_2.6.H_2O$ precursor. The pH of the solution was adjusted to 3.5 by adding a few drops of diluted HNO_3. The mixture was heated to 90 °C, then a solution of urea in 3 mL of water was added. After 18 hr, the slurry was cooled to room temperature and filtered. The coated support was thoroughly washed with deionized water and dried at 120 °C for 24 hr. After cooling to room temperature, subsequent gradual heating treatment under nitrogen flow at a heating rate of 3 °C min^{-1} to 500 °C for 4 hr was performed.

2.4.3. Hydrothermal method

The metal precursor ($Co(NO_3)_2.6.H_2O$) and urea were dissolved in 80 ml deionized water then transferred into a 100 mL teflon lined stainless steel autoclave, a disc of ACM was added as growth substrate. Afterwards, the autoclave was sealed and heated to 100 °C for 5 hr, and allowed to cool naturally to room temperature. After being washed sufficiently and ultra-sonicated for 2 min, the carbon coated substrates with catalyst precursors was annealed under nitrogen atmosphere at a heating rate of 2 °C min^{-1} to 300 °C for 2 hr. Table 2 summarizes the developed adsorbents.

Table 2
Prepared and impregnated ACM through different methods of synthesis

Metal precursor	Pore Impregnation method	Deposition precipitation method	Hydrothermal method
$Co(NO_3)_2.6.H_2O$	IM-Co_3O_4/ACM	DP-Co_3O_4/ ACM	HM-Co_3O_4/ ACM

1. ACM= activated carbon monolith

2.5 Characterization of HM-Co_3O_4/ACM

The Surface functional groups of HM-Co_3O_4/ACM was examined using Thermo Nicolet AES0200682 Fourier transform infrared (FTIR) spectroscopy which consisted of liquid nitrogen cooled mercury-cadmium-telluride detector and a spectra tech diffuse reflectance accessory.

2.6 Catalyst activity

Fixed bed adsorber made with stainless steel reactor with 10 mm internal diameter was used to prevent corrosion by corrosive gases such as SO_2. Schematic diagram of the experimental setup is shown in fig.1. The adsorbent was crashed in accordance with the work of [19] prior to catalyst test and about 1g of Co_3O_4/ACM adsorbent was placed in the center of the flue gas adsorber, sealed by quartz wool then preheated with N_2 at 120 °C for 30 min before switching to the reactant stream for activity measurement, activity test of simultaneous SO_2/NOx removal was carried out under atmospheric pressure similar to the work of [20]. Stream of flue gas was produced by burning of coal in a vertical tubular furnace at 900 °C to simulate the real life industrial flue gas production and the gas was passed through the adsorbent at flow rate of 10 ml/min. The influent and effluent concentrations of SO_2 and NO_x were simultaneously measured using flue gas analyzer (T-350, Testo Company, Germany). Unlike the experimental conditions found in the literature where the inlet concentration of the simulated gases were predetermined (i.e 100, 200, 300 mg/l), in this study, the influent and effluent concentrations were continuously monitored at an interval of 2 min with flue gas analyzer one at inlet and another at the outlet, and gas flow through the adsorption column continued for an additional time after saturation time. The activity of the adsorbent towards the adsorbate is expressed by adsorption capacity, which is defined by the weight of SO_2 or NOx captured from the flue gas per gram of adsorbent. The column temperature used was 100 °C, this is because the temperature of flue gas in the industrial stack burners varies from 120 to 250 °C as stated by Liu et l. [3]. Each and every experimental run was repeated three times to increase the precision of the results and the average value was reported.

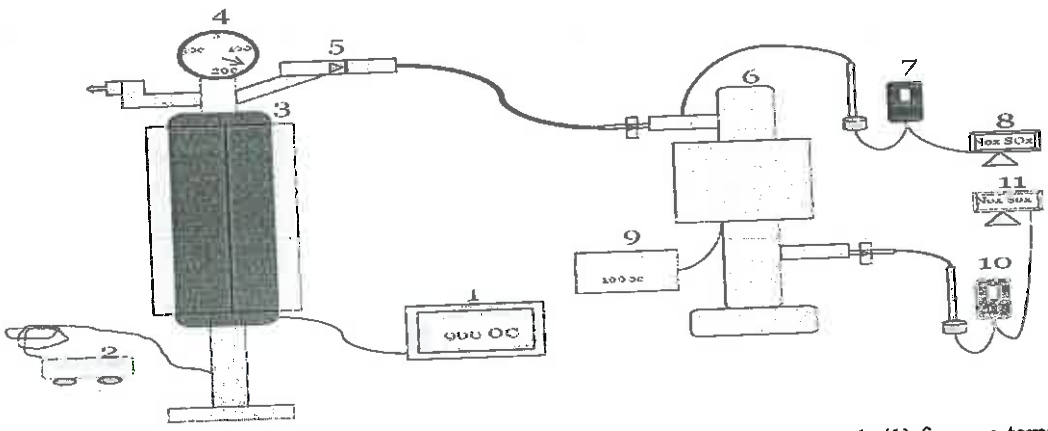

Fig. 1. Schematic of experimental setup for simultaneous SO_2 and NO_x removal: (1) furnace temperature controller, (2) air compressor, (3) vertical tubular furnace, (4) pressure gauge, (5) control valve, (6) flue gas adsober, (7) flue gas analyser I, (8) computer I, (9) flue adsorber temperature controller, (10) flue gas analyser II, (11) computer II.

3. Results and discussion

3.1. Fourier transform infrared radiation analysis (FTIR)

FTIR analysis was used to investigate the functional groups on the adsorbent surface. Functional groups are bonded to the edges of the carbon layers, acting as binding sites for catalyst support and influencing the surface chemistry of mesoporous carbon-coated monolith [6]. The fig. 2 (a), shows the FTIR spectra with display of number of adsorption peaks for the HM-Co_3O_4/ACM catalyst before catalyst test while Fig. 2 (b) presents the FTIR analysis after the catalyst test. Minute peaks were observed at 2628.82 cm^{-1} (O-H of carboxylic acid), 2361.57 cm^{-1} (C-N triple bond), 1741.42 cm^{-1} (C=O of ester stretch), 1370.24 cm^{-1} (C-O of phenolic stretch). A huge spectral range were found at 1175.42-440.87 cm^{-1} corresponding to the C-O, C-H, CH=CH_2 stretches, the same finding was reported by Malkoc et al. [21]. The presence of SO_4^{2-} and NO_3^- ions are found in the ranges of 700-450 cm^{-1}, this is similar with the work of Raghunath and Mondal [22].

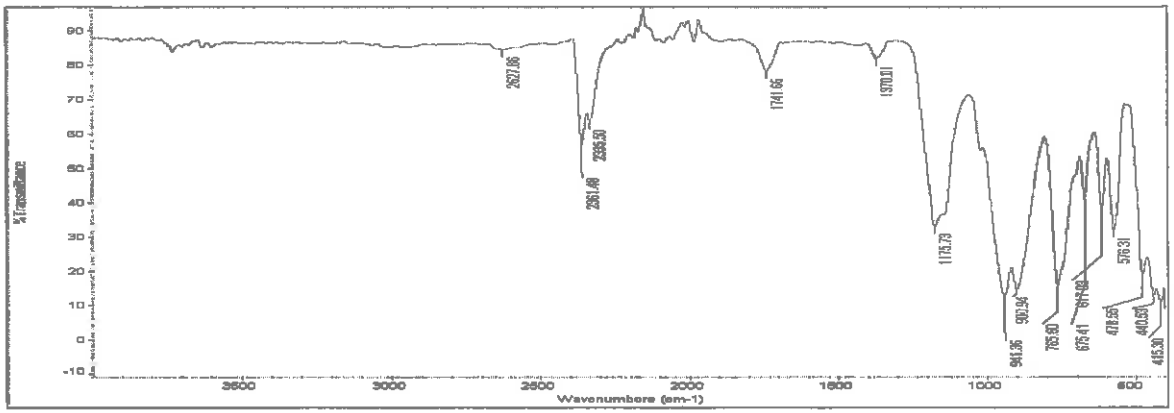

a

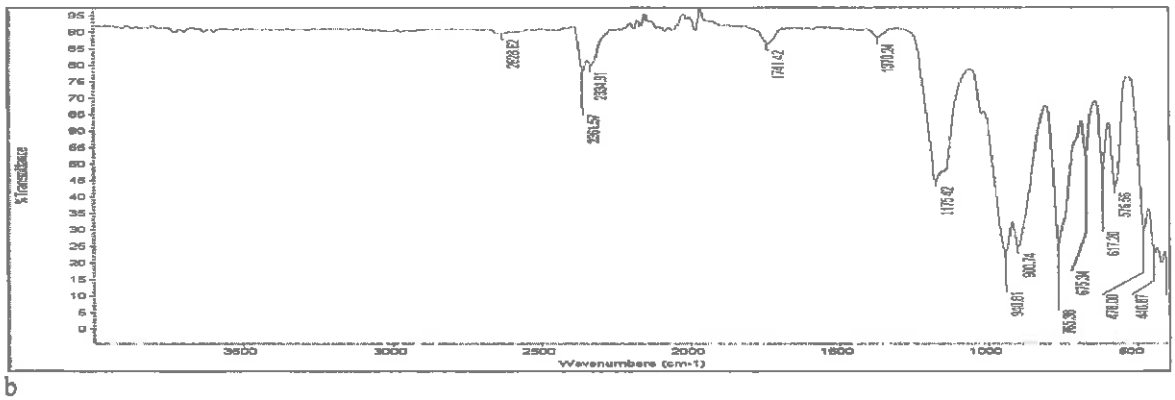

b

Fig. 2. FTIR spectra display of HM-Co_3O_4/ACM catalyst (a) before experimentation (b) after catalyst activity.

3.2. Breakthrough curve

Relationships between adsorption capacities and adsorption kinetics of the adsorbent and adsorbate can be determined through breakthrough curve studies [23]. The initial maximum SO_2/NO_x removal is mostly about 100%, to a certain time then 'breakthrough' occurs resulting in decrease in removal. The time taken for effluent concentration to reach a certain level of at least 1ppm with a fixed influent concentration is known as breakthrough time (t_b), and the performance of an adsorbent bed and adsorption capacity are often given in terms of t_b [11,24]. The saturation time (t_{sat}) is the time reached when loss of catalyst activity occurs as a result of pore blockage of the catalyst's active sites. The breakthrough information in this work was obtained under the operation conditions presented in Table 3.

Table 3
Operation conditions for catalyst activity test

Operation conditions	
Column temperature	100 °C
Pressure	1atm
Stack temperature	30 °C
NO_x concentration	50-300 ppm
SO_2 concentration	50-300 ppm
Flue gas flow rate	10 ml/min

The adsorption capacity of Co_3O_4/ACM for SO_2 and NO_x was calculated according to the adsorption breakthrough curve data from an adsorption breakthrough run which is a plot of the ratio of influent and effluent concentrations against time (C_t/C_o vs time) [25].The amount of SO_2 and NO_x adsorbed for each experiment was determined numerically from the following expression [6,26,27]:

(1)

where $_t$ is the effluent concentration, is the influent concentration, y, M, F, and t_b are the mole fraction of adsorbate in the feed, amount of the adsorbent (g), volumetric flow rate of flue gas (mL/min), and breakthrough time (min), respectively.

The continuous SO_2 and NO_x adsorption process was performed until when the effluent concentration was equal to the influent concentration (saturation point). The breakthrough curves were constructed from the experimental data and the performance of each adsorbate was evaluated from the t_b curves, similar procedure was described by Olivares et al. [28]. The figs. 3-5 show the breakthrough curves and average curves of SO_2/NO_x removal.

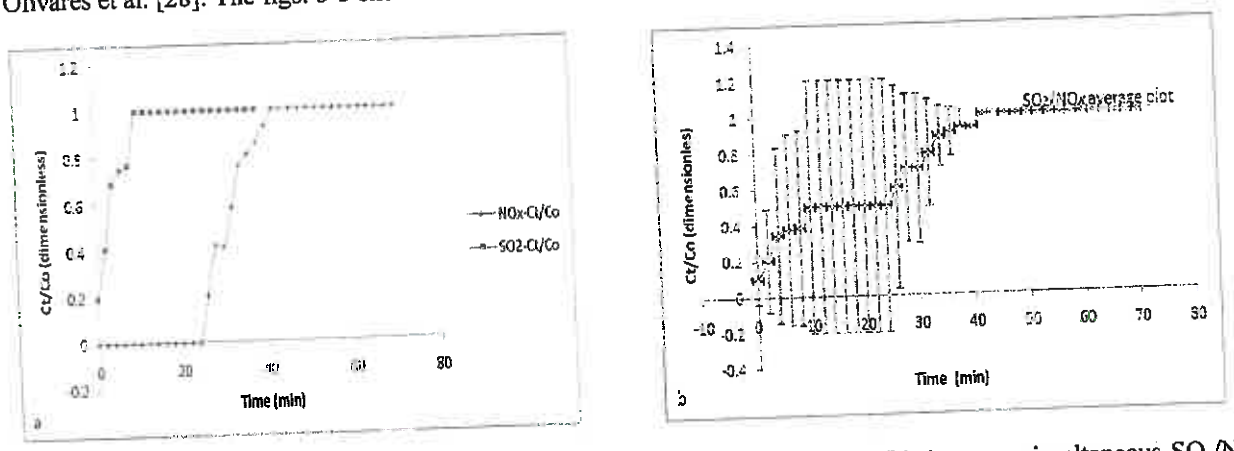

Fig. 3. Breakthrough curves of SO_2/NO_x using (a) IM-Co_3O_4/ACM adsorbent, (b) Average simultaneous SO_2/NO_x removal.

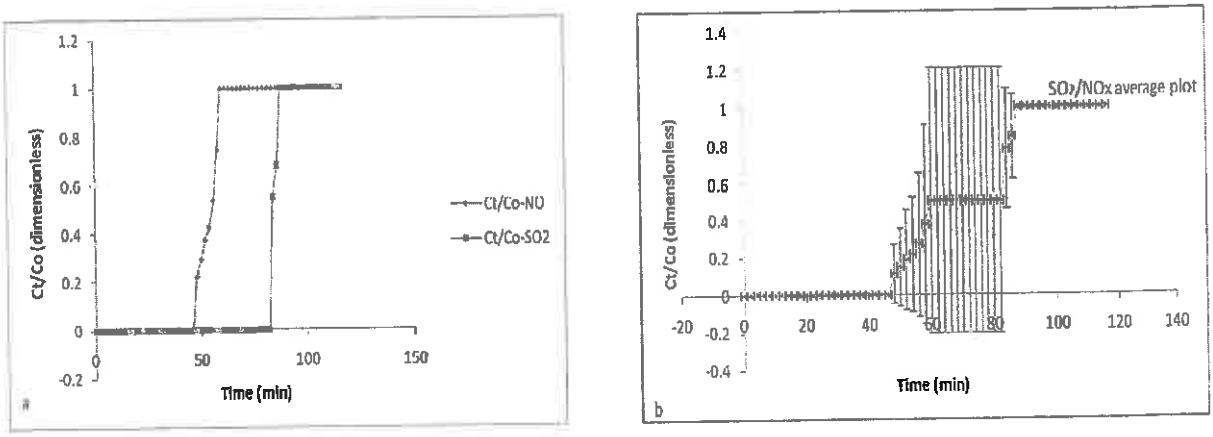

Fig. 4. Breakthrough curves of SO_2/NO_x using (a) DP-Co_3O_4/ACM adsorbent, (b) Average simultaneous SO_2/NO_x removal.

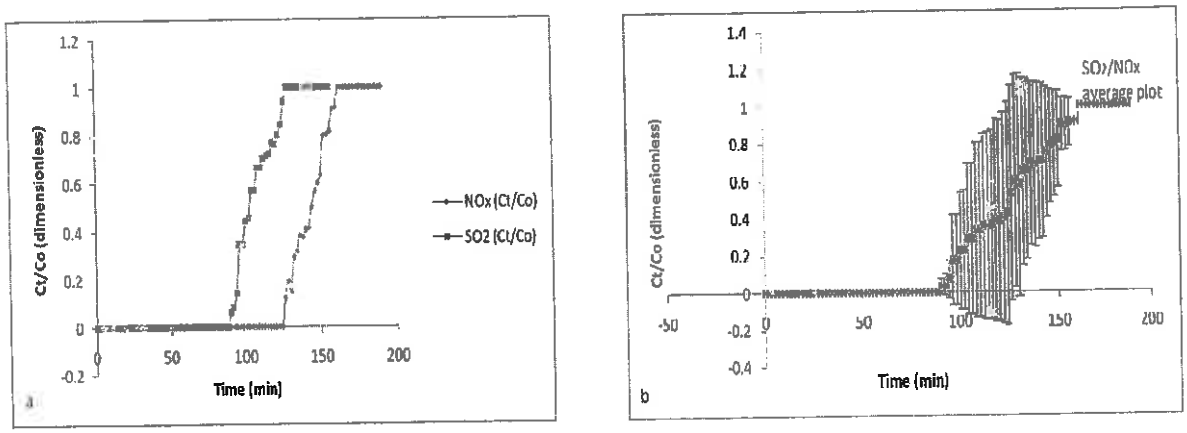

Fig. 5. Breakthrough curves of SO_2/NO_x using (a) HM-Co_3O_4/ACM adsorbent, (b) Average simultaneous SO_2/NO_x removal.

The variation in the breakthrough curves and the adsorption capacities were due to each adsorbate's ability to capture the pollutants as a result of how well it was synthesized (preparation, dispersion and calcinations processes) and the compatibility of the monolith structure with the Co_3O_4 in terms of surface interaction and active sites. The lack of smoothness in the t_d curvature stems from fluctuation in the influent concentration of the adsorbate, this can also be seen in the work of others [26]. From Fig. 3(a), there is no record of 100% SO_2 removal, exact experience was reported elsewhere [25,26], the b_t and t_{sat} were 0 and 10 min while for NO_x the b_t and t_{sat} were 24 and 42 min respectively. Fig. 4(a) depicts a better performance, with b_t and t_{sat} values for NO_x being 24 and 34 min while for SO_2 they were 42 and 44 min, indicating a dominance of SO_2 on the active sites. The longer the sorbent could maintain 100% removal of SO_2 and NO_x from flue gas, the better adsorbent it is. The performance of HM-Co_3O_4/ACM adsorbent in fig. 5 is seen to be promising because of the enhanced b_t and t_{sat} for SO_2 was 88 and 124 min, as for NO_x it was 124 and 160 min respectively. This is a good feat indicating the ability of the catalyst to endure a longer time in application consequently expecting to greatly improve the economy of the system. The maximum 100% adsorption capacity of NO_x was realized in the first 122 min thereafter, the efficiency declined down to 9% at 166 min also, 100% adsorption capacity of SO_2 was recorded for 86 min followed by steep decline in performance until finally it was 5.8% at the 122th min. The SO_2 and NO_x initial concentrations are almost the same and therefore, there was equal competition of active site. Table 4 clearly shows the adsorption capacity of the adsorbents.

Table 4
Experimental adsorption capacities and breakthrough/saturation time

Catalyst	Breakthrough time (min), SO_2 and NO_x	Saturation time (min), SO_2 and NO_x	Adsorption capacity q (mg/g), SO_2 and NO_x
HM Co_3O_4/ACM	86 and 122	124 and 160	123.1 and 130.2
DP-Co_3O_4/ACM	42 and 24	46 and 36	10.6 and 49.7
IM-Co_3O_4/ACM	0 and 24	42 and 40	17.5 and 42.3

3.3. Adsorption isotherm

To describe the SO_2 and NO_x adsorption behavior on the MO/monolith, the Langmuir and Freundlich equations were used to fit the isotherms as Zhou et al. [26] recommended. In several papers [27,28,29,30], Langmuir and Freundlich were used to correlate the experimental data.

3.3.1. The Langmuir model

The Langmuir model was based on the assumption that; (a) at maximum adsorption, there was only a monolayer of adsorbed material formed implying that molecules of adsorbate do not deposit on each other and the adsorption sites were identical, (b) the adsorbed molecules does not interact under constant temperature, (c) the surface of the adsorbent was uniform with equal adsorption sites, (d) all the adsorption occurred through the same mechanism. Langmuir equation is [31] expressed given as:

$$q_e = \frac{q_m \cdot K_L \cdot C_e}{1+K_L \cdot C_e} \quad (2)$$

where q_e is the equilibrium adsorption capacity (mg/g),C_e is the equilibrium concentration, q_m and K_L are the maximum adsorption capacity to form a complete monolayer on the surface (mg/g) and the Langmuir constant related to the energy of adsorption (bonding energy of sorption in L/g), respectively.
The linearized form of Langmuir equation is as follows:

$$\frac{Ce}{qe} = \frac{1}{q_m \cdot K_L} + \frac{Ce}{q_m} \quad (3)$$

where the slope, $1/q_m$ and intercept, $1/K_L \cdot q_m$ could be determine from plot of $\frac{Ce}{q_e}$ against C_e.
There is a characteristic of the Langmuir isotherm referred to separation factor (R_L) which is a dimensionless parameter for predicting the adsorption efficiency of the adsorption process and indicates the suitability of Langmuir isotherm as either unfavorable (R_L>1), linear (R_L=1), favorable (0 < R_L< 1) or irreversible (R_L=0) [25,32-34]. R_L can be express as:

$$R_L = \frac{1}{1+K_L \cdot Co} \quad (4)$$

where Co is the highest initial concentration of adsorbate (mg/L), and K_L (L/mg) is the Langmuir constant.

3.3.2. The Freundlich model

The adsorption on heterogeneous surface through a multilayer adsorption mechanism is described by Freundlich isotherm [29]. The following postulations were considered in formulating the Freundlich model [35]; (a) adsorption surface is energetically heterogeneous and (b) the adsorbed amount increases with the concentration. Freundlich model is expressed by the relationship as [26]:

$$q_e = k_f C_e^{1/n} \quad (5)$$

where k_f is Freundlich constant, $1/n$ is the heterogeneity factor and describes adsorption capacity, its value becoming more heterogeneous as it gets farther to one, n has a value greater than unity [23,26,31]. The range of favorable adsorption is $1 < n < 10$ [6,29]or $1/n$ is in the range of 0.1–1.0 [33]. The surface heterogeneity is enhanced with high

values of $1/n$ however, when, n is small, the adsorption affinity increases [34]. The linearized form of Freudlich model is:

$$logq_e = logk_f + \frac{1}{n} logC_e \quad (6)$$

k_f, n and r^2 can be determined from the slope, intercept and correlation coefficient by plotting $\ln(q_e)$ versus $\ln(C_e)$ [29,35].

3.3.3. Mechanisms and removal efficiency

Three steps were involved in the reaction of SO_2/NO_x removal on the adsorbate (Co_3O_4/ACM); (1) chemisorption of SO_2 and NO_x on the catalyst surface, (2) transfer of oxygen from catalytic sites to the reactive sites and (3) desorption of oxygen from the carbon surface [36]. The mechanism of adsorption of NO_x and SO_2 on the active sites of the adsorbent can be written as the mechanism on the active site during the adsorption [37]:

$$NO + O_2* + SO_2* \rightarrow [(NO_2)(SO_2)]* + * \quad (7)$$

$$NO_2* + SO_2* + SO_3* + NO + * \quad (8)$$

Asterisk stands for adsorbed molecules on the active sites. The water vapor in the flue gas combines with the SO_2 molecules to form $SO_2 \cdot H_2O$ which dissociates to H^+, HSO_3^-, and SO_3^{2-}, and these ions react with O_2 to form H_2SO_4, this is represented as [37,38]:

$$SO_2 + 1/2O_2 + H_2O + C \rightarrow C\text{–}H_2SO_4 \quad (9)$$

SO_2 gas inhibits the adsorption of NO_x gas since it has slightly larger molecule and compete for O_2 [39], in this study, several reasons can be associated with high NO_x adsorption capacity in the simultaneous SO_2/NO_x removal;

1. Adsorption capacity and removal efficiency are gas composition concentration dependant parameters [39,40]. Sumathi et al. [37] examined the concentration dependence by reducing SO_2 concentration from 2500-1000 ppm and increasing NO from 300-700 ppm then conclude that with increase in NO concentration, NO adsorption was more favored. Dahlan et al. [41] used rice husk ash (RHA) impregnated with metal oxides and carried out catalyst activity with simulated flue gas (2000 ppm, SO_2 and 500 ppm NO) and reported that lower NO concentration resulted to lower NO removal since the SO_2 dominate the active site.
2. The core adsorbent material, preparation and characteristics defines the SO_2 and NO_x removal capabilities [42]. Monolith was found to have mesoporous pores [43], when its surface area is oxidized using acid treatment, the dispersion of active component (MO) was greatly improved to accommodate and provide abundant actives for SO_2 and NO removal. The same argument was established by many authors [12 ,44].
3. The temperature of operation influences the SO_2 and NO_x diffusion on the pores. Some authors [37] reported that higher temperature (150-200 °C) favors SO_2 adsorption because boiling point of SO_2 is higher than that of NO_x so that NO_x can diffuses more easily at low temperatures (100 °C) than SO_2. Molecules with higher boiling point will create more Van der Waals attractive forces and the ones with lower boiling point will only have weak intermolecular interactions thus the physically adsorbed NO_x is easily being replaced and desorbed by SO_2 at higher temperature [39]. One of the reasons why Co_3O_4/ACM adosorbent has the property of preferential adsorption of NO_x in the presence of both SO_2 and NO_x, was the low column temperature (100 °C) used, Zhao et al. [7] arrived at the same conclusion.
4. The presence of high O_2 in the flue gas can improve NO_x removal [45,46]. In most researches, 10 % O_2 were used in the simulated flue gas [10,18,47] in this study the flue gas generated was recorded to have about 20% O_2.
5. Water vapor is usually added to simulated flue gases to increase the relative humidity of the adsorbate and consequently enhances removal of NO, the procedure and description of such studies can found in the literature [37,41]. It was observed and demostrated [37], that relative humidity 15% was optimum in simultaneous SO_2/NO_x removal. Studies have shown that 2-18% of H_2O is present in flue gas [41] and can influence the SO_2 and NO removal.

The mechanism for the adsorption of SO_2 and NO_x in the presence of oxygen and water is described according to following equations [48];

(10)

$SO_{2(gas)} \rightarrow SO_{2(ads)}$ (11)

$H_2O_{(gas)} \rightarrow H_2O_{(ads)}$ (12)

$1/2O_{2\ (gas)} \rightarrow O_{(ads)}$ (13)

$SO_{2(ads)} + O_{(ads)} \rightarrow SO_{3(ads)}$ (14)

$SO_{3(ads)} + H_2O_{(ads)} \rightarrow HSO_{4(ads)}$ (15)

$H_2SO_{4(ads)} + {}_nH_2O_{(ads)} \rightarrow H_2SO_4{}_nH_2O_{(ads)}$ (16)

$Z^* + 1/2O_2 \rightarrow Z(O)$ (17)

$Z(O) + NO \rightarrow Z^*(O) + NO_2$

Active center that reacts with oxygen is represented by Z* (possibly, nitrogen functionalities), to form a reactive surface intermediate Z(O).The simultaneous SO_2/NO_x removal efficiencies is defined as [1]:

(18)

where, is the removal efficiency (%).

The applicability of an isotherm can be determined through the coefficient of determination (r^2) [33]. Freundlich model showed r^2 value of 0.527 for SO_2 and unfavorable n value of 0.640 compared to NO_x having r^2 value of 0.7250 and n value of 0.102 in the case of using HM-Co_3O_4/ACM adsorbent.

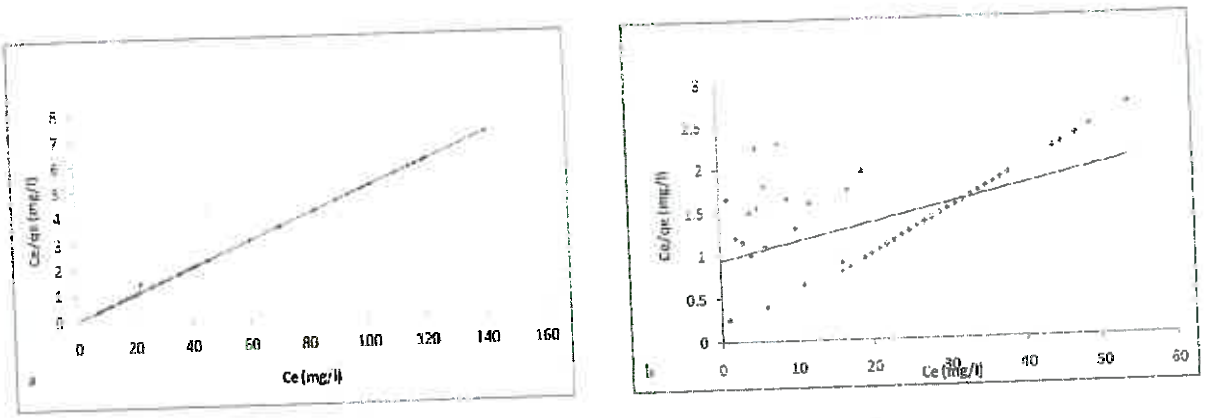

Fig. 6. Langmuir isotherm evaluation of (a) NO_x and (b) SO_2, using HM-Co_3O_4/ACM adsorbent

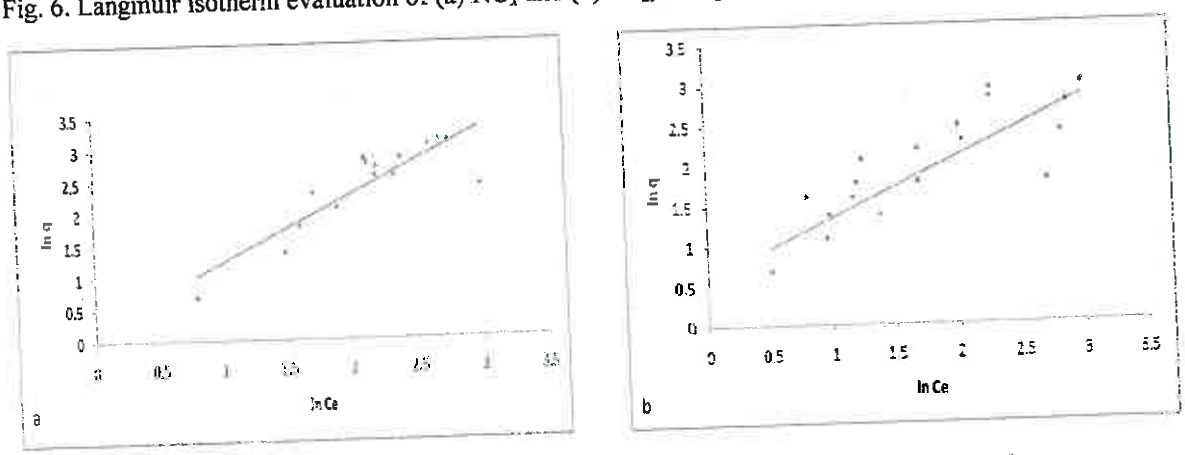

Fig. 7. Freundlich isotherm evaluation of (a) NO_x and (b) SO_2, using HM-Co_3O_4/ACM adsorbent

The r^2 value of SO_2 was low for Langmuir model (0.2710). Interestingly, the r^2 value of the NO_x was 0.9999 in the Langmuir model therefore, it supersedes the characteristics of the Freundlich mode and hence, the Langmuir

isotherm model is more suitable to explicate the correlation of experimental results, similar result was reported [35]. Moreover, the evidence of Langmuir model suitability was shown by the R_L values of < 1, calculated for NO_x, it was found to be 0.0097 and 0.3277 for SO_2 respectively.

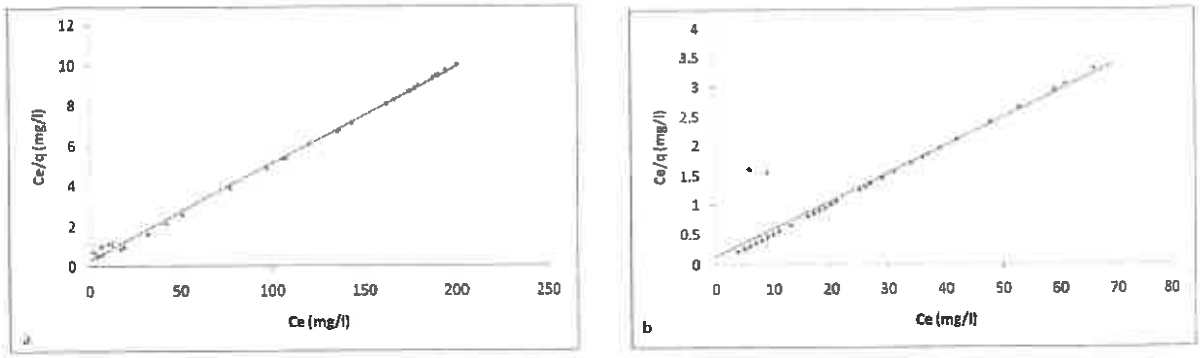

Fig. 8. Langmuir isotherm evaluation of (a) NO_x and (b) SO_2, using DP-Co_3O_4/ACM adsorbent

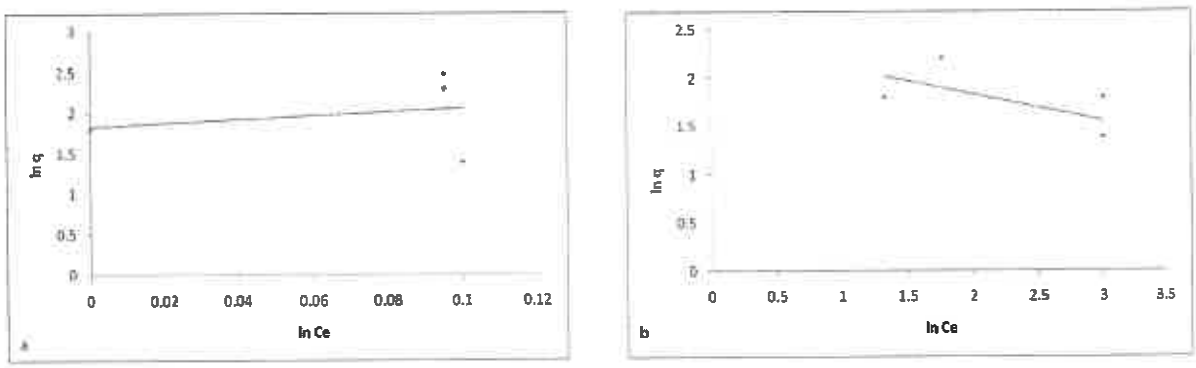

Fig. 9. Freundlich isotherm evaluation of (a) NO_x and (b) SO_2, using DP-Co_3O_4/ACM adsorbent

Figs. 8 (a) and (b) showed that for NO_x and SO_2, the r^2 were 0.9997 and 0.9998 respectively, with maximum adsorption capacities of 21.8 and 20.4 mg/g for NO_x and SO_2. The *n* value and r^2 of SO_2 (10.98 and 0.0881) and NO_x (1.82 and 0.045) indicated that Freundlich isotherm could not represent the adsorption isotherm of DP-Co_3O_4/ACM adsorbent but Langmuir isotherm dominates and fitted well to described the adsorbent, this result is in agreement with the work of Sumathi et al. [29]. The calculated R_L value for NO_x and SO_2 were found to be 0.0641 and 0.0143 respectively, indicating the applicability of Langmuir model for the correlation of the experimental results of SO_2 and NO_x adsorption on DP-Co_3O_4/ACM, similar work was reported in the literature [34].

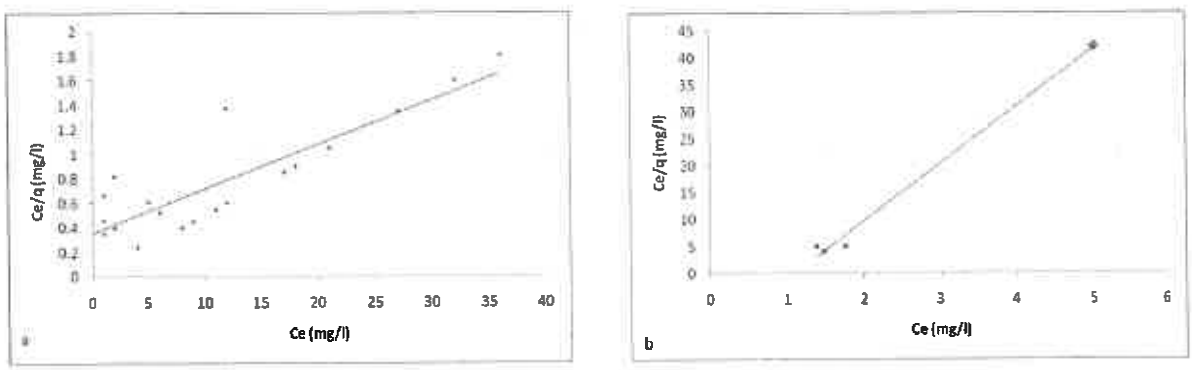

Fig. 10. Langmuir isotherm evaluation of (a) NO_x and (b) SO_2, using IM-Co_3O_4/ACM adsorbent

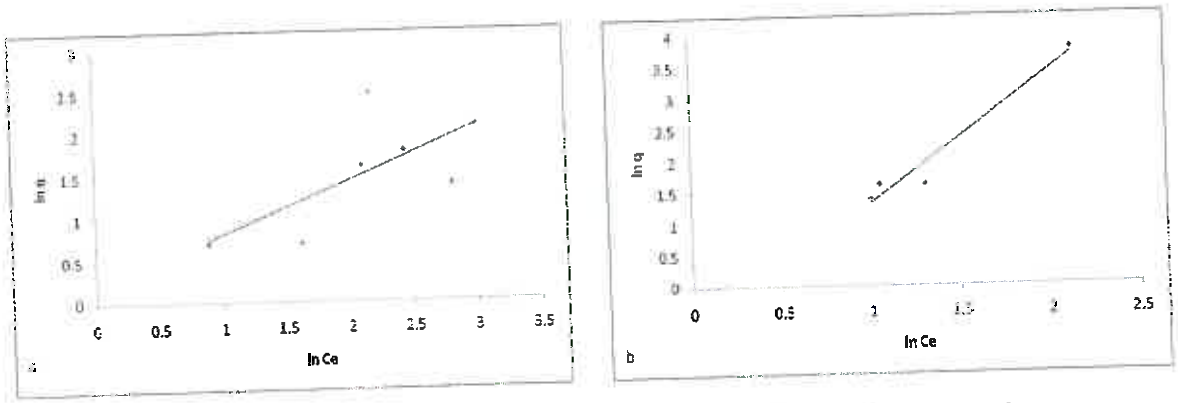

Fig. 11. Freundlich isotherm evaluation of (a) NO_x and (b) SO_2, using IM-Co_3O_4/ACM adsorbent

The maximum adsorption capacity of NO_x on the IM-Co_3O_4/ACM catalyst was up to 27.7 mg/g with r^2 value of 0.7510 also, the r^2 value for SO_2 was 0.9991 with low maximum adsorption capacity of 0.09 mg/g in case of the Langmuir isotherm. Furthermore, n values for NO_x and SO_2 (0.179 and 0.758) with r^2 values (0.454 and 0.0956) in the Freundlich isotherm evaluated were indications that the Langmuir model described the experimental data better. R_L value for NO_x was 0.0013 and SO_2 was 0.0028 respectively. Table 5, shows the experimental and literature numerical parameters of adsorption capacities and constants of Langmuir/Freundlich and fitting comparison.

Table 5
Calculated and literature numerical parameters with constants of Langmuir/Freundlich for SO_2 and NO_x

Adsorbent/ source of flue gas	C_o (mg/l), SO_2/NO_x	q (mg/g) SO_2/NO_x	LP	SO_2	NO_x	FP	SO_2	NO_x	Sources
Ce/PSAC/simulated flue gas	1000/500 ppm	89.33 and 3.17	q_m	153.85	6.92	k_f	0.0229	107.54	[59]
			k_L	0.00149	0.00156	n	0.4208	0.7168	
			r^2	0.992	0.987	r^2	0.9175	0.9903	
zeolite N_aY/ simulated flue gas	2000/1000 ppm = 1/1 (v%)	-	q_m	5.398	0.0621	k_f	0.0002	0.0001	[4]
			k_L	8.972	33.91	n	1.219	1.811	
			r^2	0.9941	0.9508	r^2	0.9976	0.9724	
Zeolite N_aX/simulated flue gas	2000/1000 ppm = 1/1 (v%)	-	q_m	6.473	0.1581	k_f	0.0009	0.0008	[4]
			k_L	17.61	48.52	n	1.34	2.234	
			r^2	0.9962	0.9788	r^2	0.9948	0.9958	
zeolite C_aA/ simulated flue gas	2000/1000 ppm = 1/1 (v%)	-	q_m	2.125	0.1644	k_f	0.0117	0.0008	[4]
			k_L	72.58	47.41	n	2.165	2.202	
			r^2	0.9921	0.9782	r^2	0.9552	0.9980	
ACF/ simulated flue gas	1/1 (v%)	-	q_m	9.086	5.546	k_f	0.454	0.088	[58]
			k_L	25.03	8.350	$1/n$	0.623	0.744	
			r^2	0.991	0.993	r^2	0.998	0.996	
HM Co_3O_4/ ACM / flue gas from coal	50-300 ppm	122.53 and 132.75	q_m	50	20.4	k_f	0.737	1.079	This study
			k_L	0.0206	0.845	n	0.640	0.102	
			r^2	0.2710	0.9999	r^2	0.527	0.7250	
DP-Co_3O_4/ ACM / flue gas from coal	50-300 ppm	10.6 and 49.7	q_m	20.4	20.8	k_f	0.531	2.238	This study
			k_L	0.3673	0.1684	n	10.98	1.825	
			r^2	0.9998	0.9997	r^2	0.0881	0.0450	
IM-Co_3O_4/ ACM / flue gas from coal	50-300 ppm	17.63 and 59.07	q_m	0.09	27.7	k_f	2.076	0.630	This study
			k_L	1.08	9.8	n	0.758	0.179	
			r^2	0.9991	0.7510	r^2	0.0956	0.4540	

2. Palm shell activated carbon supported with cerium = Ce/PSAC, 3. Activated Carbon Fiber = ACF, 4. LP=Langmuir parameter, 5. FP=Freundlich parameter

Due to the high NO_x adsorption affinity on the Co_3O_4/ACM and the high amount of NO_x in the flue gas compared to the simulated flue gas used in literature (low NO_x), it was found that NO_x adsorption was at equal contention with SO_2 with the Co_3O_4/ACM irrespective of the synthesis method. The figs. 12 (a-c) presents the deactivation process as a function of time. The experimental result depicts the efficient simultaneous SO_2 and NO_x removal on adsobate which was partly as a result of Co_3O_4 precursor support and without doubt it was the reason for enhanced saturation time and high adsorption capacity. The physisorption of SO_2 occurs on the micropores but the dispersed of Co_3O_4 of nanoparticles on the support partially blocks the micropores yet the nanoparticles are responsible for the chemisorptions of SO_2, and avail more active sites.

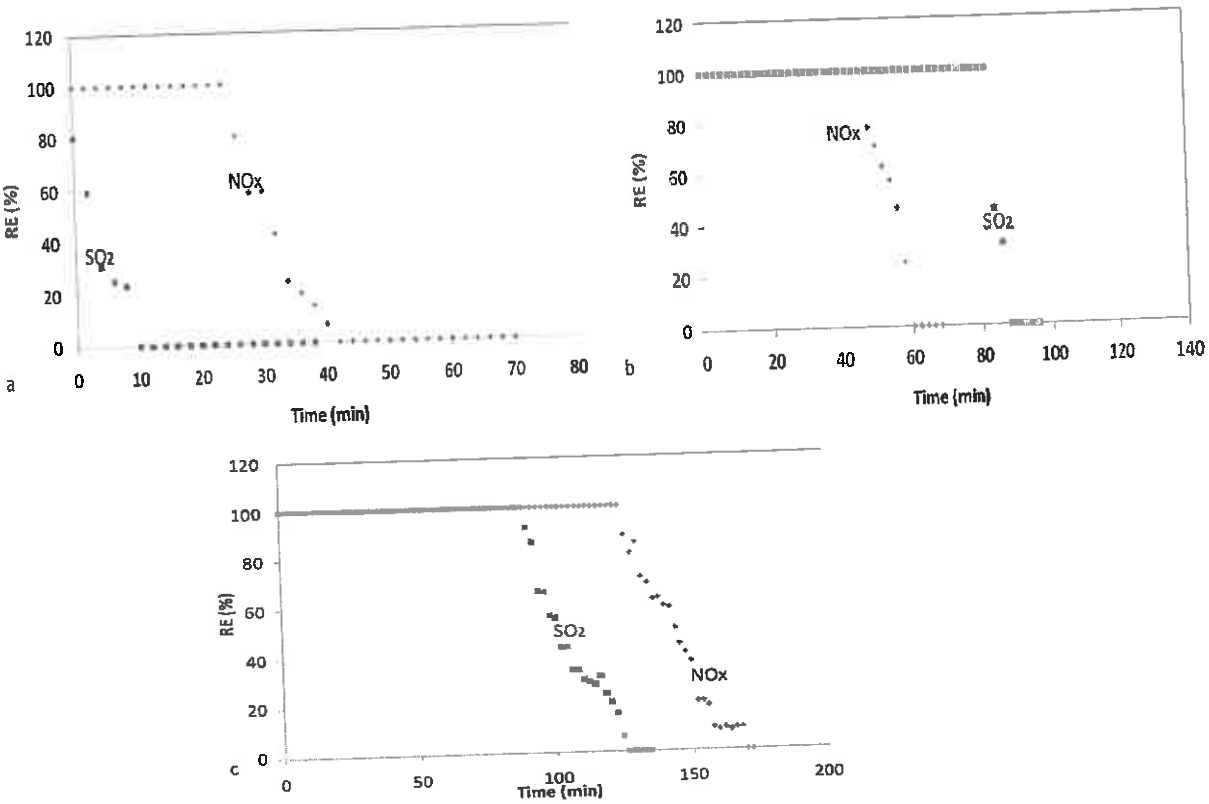

Fig. 12. Removal efficiency (%) over time (a) IM-Co_3O_4/ACM (b) DP-Co_3O_4/ACM (c) HM-Co_3O_4/ACM

The adsorbed pollutants and temperature of the column were manifested on the loss of catalyst activity and exhibit coarse surface and particle hardness on the adsorbent.

4. Conclusion

In this study, three different synthesis methods were used to develop an activated carbon monolith supported metal oxide catalyst (Co_3O_4/monolith) and applied for the simultaneous SO_2 and NO_x removal from generated flue gas. According to the breakthrough experimental results, the best simultaneous SO_2 and NO_x removal was achieved through hydrothermal synthesized adsorbent (HM-Co_3O_4/ACM) with adsorption capacities for SO_2 and NO_x values of 123.1mg/g and 130.2 mg/g. The adsorbent's unique ability to high NO_x adsorption capacity has been demonstrated as promising which no literature work has reported in this regard. It was concluded that the overall adsorption process was described by the Langmuir adsorption isotherm in HM-Co_3O_4/ACM and DP-Co_3O_4/ACM and IM-Co_3O_4/ACM adsorbents.

Acknowledgements

The authors would like to gratefully acknowledge Universiti Putra Malysia (UPM) for the financial support of this work (via Geran Putra UPM/9515201).

References

[1] J. Ding, Q. Zhong, S. Zhang, F. Song, Y. Bu, Simultaneous removal of NO_x and SO_2 from coal-fired flue gas by catalytic oxidation-removal process with H_2O_2, Chemical Engineering Journal 243 (2014) 176-182.

[2] B. Guan, R. Zhan, H. Lin, Z. Huang, Review of state of the art technologies of selective catalytic reduction of NO_x from diesel engine exhaust, Applied Thermal Engineering 66 (2014) 395-414.

[3] Y. Liu, T.M. Bisson, H. Yang, Z. Xu, Recent developments in novel sorbents for flue gas clean up, Fuel Processing Technology 91 (2010) 1175-1197.

[4] I. Nova, A. Beretta, G. Groppi, L. Lietti, E. Tronconi, and P. Forzatti, Monolithic Catalysts for NO, Structured Catalysts and Reactors (2006) 171-214.

[5] S. Colussi, M. Boaro, L. Rogatis, A. Pappacena, C. Leitenburgh, J. Llora, A. Trovarelli, Room temperature oxidation of formaldehyde on Pt-based catalysts: A comparison between ceria and other supports (TiO_2, Al_2O_3 and ZrO_2), Catal. Today 253 (2015) 163-171.

[6] S. Hosseini, E. Marahel, I. Bayesti, A. Abbasi, L.C. Abdullah, T.S.Y. Choong, CO_2 adsorption on modified carbon coated monolith: effect of surface modification by using alkaline solutions, Applied Surface Science 324 (2015) 569-575.

[7] Y. Zhao, G. Hu, Z. Sun, J. Yang, Simultaneous removal of SO_2 and NO_2 on r-Al_2O_3 absorbents loaded with sodium humate and ammonia water, Energy Fuels 25 (2011) 2927-2931.

[8] S. Hosseini, M.A. Khan, M.R. Malekbala, W. Cheah, T.S.Y. Choong, Carbon coated monolith, a mesoporous material for the removal of methyl orange from aqueous phase: Adsorption and desorption studies, Chemical Engineering Journal 171 (2011) 1124- 1131.

[9] A. D. Browski, Adsorption from theory to practice, Advances in Colloid and Interface Science 93 (2001) 135-224.

[10] H.B. Fang, J.T. Zhao, Y.T. Fang, J.J. Huang, Y. Wanga, Selective oxidation of hydrogen sulfide to sulfur over activated carbon-supported metal oxides, Fuel 108 (2013) 143-148.

[11] Y. Wang, Z. Huang, Z.Liu, Q. Liu, A novel activated carbon honeycomb catalyst for simultaneous SO_2 and NO removal at low temperatures, Letters to the Editor/Carbon, 42 (2004) 423-460.

[12] S. Hosseini, S. AbdulRashid, A. Abbasi, F. E. Babadi, L. C. Abdullah,T.S.Y.Choong, Effect of catalyst and substrate on growth characteristics of carbon nanofiber on to honeycomb monolith, Journal of the Taiwan Institute of Chemical Engineers, 59 (2016) 440-449.

[13] T. Vergunst, F. Kapteijn, and J. A. Moulijn, Monolithic catalysts non-uniform active phase distribution by impregnation, Appl. Catal. A Gen. 213 (2001) 179-187.

[14] M. Assebban , Z.Y. Tian, A. El Kasmi, N. Bahlawane, S. Harti, T.Chafik, Catalytic complete oxidation of acetylene and propene over clay versus cordierite honeycomb monoliths without and with chemical vapor deposited cobalt oxide, Chemical Engineering Journal 262 (2015) 1252-1259.

[15] L. Zhigang, L. Aibin, J.I.A. Meiru, L. Xueyi, Experimental and Kinetic Study of Selective Catalytic Reduction of NO with NH_3 over CuO/Al_2O_3/Cordierite Catalyst, Chinese Journal of Chemical Engineering 18 (2010) 721-729.

[16] F.C. Patcas, G.I. Garrido, B.K.Czarnetzki, CO oxidation over structured carriers: A comparison of ceramic foams, honeycombs and beads, Chemical Engineering Science 62 (2007) 3984-3990.

[17] P. Avila, M. Montes, E.E. Mir´o, Monolithic reactors for environmental applications a review on preparation technologies, Chemical Engineering Journal 109 (2005) 11-36.

[18] Y. Hou, R. Zhang, X. Han, Z. Huang, Y. Cui, The mechanism of CO regeneration on V_2O_5/AC catalyst and sulfur recovery, Chemical Engineering Journal 316 (2017) 744-750.

[19] C. Gaudillere, J.J. González, A. Chica, J.M. Serra, YSZ monoliths promoted with Co as catalysts for the production of H_2 by steam reforming of ethanol, Applied Catalysis A: General 538 (2017) 165–173

[20] Y. Zuo, H. Yi, X.Tang Metal-modified active coke for simultaneous removal of SO_2 and NO_x from sintering flue gas, Energy and Fuels (2014) 1-35.

[21] E. Malkoc, Y. Nuhoglu, Y. Abali, Cr(VI) adsorption by waste acorn of *Quercus ithaburensis* in fixed beds: Prediction of breakthrough curves, Chemical Engineering Journal 119 (2006) 61-68.

[22] C. V. Raghunath, M. K. Mondal, Experimental scale multi component absorption of SO_2 and NO by NH_3/NaClO scrubbing, Chemical Engineering Journal 314 (2017) 537-547.

[23] W.T. Tsai, C.Y. Chang, C.Y. Ho, L.Y. Chen, Adsorption properties and breakthrough model of 1,1-dichloro-1-fluoroethane on activated carbons, Journal of Hazardous Materials B 69 (1999) 53-66.

[24] S. Rezaei, M.Ophelia, D. Jarligo, L. Wu, S. M. Kuznicki, Break through performances of metal-exchanged nano titanate ETS-2 adsorbents for room temperature desulfurization, Chemical Engineering Science 123 (2015) 444-449.

[25] S. Ghorai, K.K. Pant, Equilibrium, kinetics and breakthrough studies for adsorption of fluoride on activated alumina, Separation and Purification Technology 42 (2005) 265-271.

[26] X. Zhou, H. Yi, X. Tang, H. Deng, H. Liu, Thermodynamics for the adsorption of SO_2, NO and CO_2 from flue gas on activated carbon fiber, Chemical Engineering Journal 200-202 (2012) 399-404.

[27] S. Sumathi, S. Bhatia, K.T. Lee and A.R. Mohamed, Adsorption isotherm models and properties of SO_2 and NO removal by palm shell activated carbon supported with cerium (Ce/PSAC), Chemical Engineering Journal, 162 (2010) 194-200.

[28] J.C. Olivares, C.P. Alonso a, C.B. Díaz , F.U. Nuñez, M.C. Chaparro-Mercado, B. Bilyeu, Modeling of lead (II) biosorption by residue of allspice in a fixed-bed Column, Chemical Engineering Journal 228 (2013) 21-27.

[29] Y. P. Teoh, M. A. Khan, T. S.Y. Choong, Kinetic and isotherm studies for lead adsorption from aqueous phase on carbon coated monolith, Chemical Engineering Journal 217 (2013) 248-255.

[30] F. Ghorbani, H. Younesi, S. M. Ghasempouri, A. A. Zinatizadeh, M. Amini, A. Daneshi, Application of response surface methodology for optimization of cadmium biosorption in an aqueous solution by *Saccharomyces cerevisiae*, Chemical Engineering Journal 145 (2008) 267-275.

[31] Muhammad, M.A. Khana, T.S.Y. Choong, T.G. Chuaha, R.Yunus,Y.H.T. Yap, Desorption of β-carotene from mesoporous carbon coated monolith: Isotherm, kinetics and regeneration studies, Chemical Engineering Journal 173 (2011) 474-479.

[32] K.A. Shroff, V.K. Vaidya, Kinetics and equilibrium studies on biosorption of nickel from aqueous solution by dead fungal biomass of *Mucor hiemalis*, Chemical Engineering Journal 171 (2011) 1234-1245.

[33] Muhammad, T.S.Y. Choong, T.G. Chuah, R. Yunus, Y.H.T. Yap, Adsorption of β-carotene onto mesoporous carbon coated monolith in isopropyl alcohol and n-hexane solution: equilibrium and thermodynamic study, Chemical Engineering Journal 164 (2010) 178-182.

[34] A. Abdedayem, M. Guiza, A. Ouederni, Copper supported on porous activated carbon obtained by wetness impregnation: Effect of preparation conditions on the ozonation catalyst's characteristics, C. R. Chimie 18 (2015) 100-109.

[35] K.H. Park, M.S. Balathanigaimani, W.G. Shim, J.W. Lee, H. Moon, Adsorption characteristics of phenol on novel corn grain-based activated carbons, Microporous and Mesoporous Materials 127 (2010) 1-8.

[36] S. Sumathi, S. Bhatia, K.T. Lee, A.R. Mohamed, Performance of shell activated carbon impregnated with CeO_2 and V_2O_5 catalyst in simultaneous removal of SO_2 and NO, Journal of applied science 10 (2010) 1052-1059.

[37] S. Sumathi, S. Bhatia, K.T. Lee, A.R. Mohamed, Cerium impregnated palm shell activated carbon (Ce/PSAC) sorbent for simultaneous removal of SO_2 and NO-Process study, Chemical Engineering Journal 162 (2010) 51-57.

[38] Y. Wang, Z. Liu, L. Zhan, Z. Huang, Q. Liu, J. Ma, Performance of an activated carbon honeycomb supported V_2O_5 catalyst in simultaneous SO_2 and NO removal, Chemical Engineering Science 59 (2004) 5283-5290.

[39] S. Sumathi, S. Bhatia, K.T. Lee, A.R. Mohamed, Selection of best impregnated palm shell activated carbon (PSAC) for simultaneous removal of SO_2 and NO_x, Journal of Hazardous Materials 176 (2010) 1093-1096.

[40] T. Qiang, Z. Zhigang, Z.Wenpei, C. Zidong, SO_2 and NO selective adsorption properties of coal-based activated carbons, Fuel 84 (2005) 461-465.

[41] I. Dahlan, K. T. Lee, A. H. Kamaruddin, A. Mohamed, Selection of metal oxides in the preparation of rice husk ash (RHA)/CaO sorbent for simultaneous SO_2 and NO removal,
Journal of Hazardous Materials 166 (2009) 1556-1559.

[42] M.E. Ga´lvez , M.J. La´zaro, R. Moliner, Novel activated carbon-based catalyst for the selective catalytic reduction of nitrogen oxide, Catalysis Today 102-103 (2005) 142-147.

[43] M.J. La´zaro, A. Boyano, M.E. Ga´lvez, M.T. Izquierdo, E. Garcı´a-Bordeje´, C. Ruiz, R. Juan, R. Moliner, Novel carbon based catalysts for the reduction of NO: Influence of support precursors and active phase loading, Catalysis Today 137 (2008) 215-221.

[44] M. T. Kreutzer, P. Du, J. J. Heiszwolf, F. Kapteijn, J. A. Moulijn, Mass transfer characteristics of three-phase monolith reactors, Chemical Engineering Science 56 (2001) 6015-6023.

[45] H. Zhang, H.Tong, S. Wang, Y. Zhuo, C. Chen, X. Xu, Simultaneous Removal of SO_2 and NO from Flue Gas with Calcium-Based Sorbent at Low Temperature, Ind. Eng. Chem. Res. 45 (2006) 6099-6103.

[46] C.F. Liu, S.M. Shih, Effects of flue gas components on the reaction of $Ca(OH)_2$ with SO_2. Ind. Eng. Chem. Res. 45 (2006) 8765-8769.

[47] Y. Liu, P. Ning, K. Lia, L. Tanga, J. Hao, X. Songa, G. Zhanga, C. Wanga, Simultaneous Removal of NO_x and SO_2 by Low-temperature Selective Catalytic Reduction over Modified Activated Carbon Catalysts, Russian Journal of Physical Chemistry A 91(2017) 490-499.

[48] Z.S. Liu, Adsorption of SO2 and NO from incineration flue gas onto activated carbon fibers, Waste Management 28 (2008) 2329-2335.

b) Paper

BioLEAGUES
www.bioleagues.com

3rd GoGreen Summit
23rd-24th, March 2018 at Manila, Philippines

Breakthrough Studies of Co3O4 Supported Activated Carbon Monolith for Simultaneous SO2/NOx Removal from Flue Gas

W.A. Wan Ab Karim Ghani
Department of Chemical & Environmental Engineering, Universiti Putra Malaysia, 43400 UPM, Serdang, Selangor, Malaysia

S. Kiman
Department of Chemical & Environmental Engineering, Universiti Putra Malaysia, 43400 UPM, Serdang, Selangor, Malaysia

T.S.Y. Choong
Department of Chemical & Environmental Engineering, Universiti Putra Malaysia, 43400 UPM, Serdang, Selangor, Malaysia

R. Umer
Department of Chemical & Environmental Engineering, Universiti Putra Malaysia, 43400 UPM, Serdang, Selangor, Malaysia

Abstract

This work investigates the deposition precipitation, pore volume impregnation and hydrothermal methods in the synthesis of activated carbon monolith with metal oxide (Co_3O_4). The catalytic activity was carried out for the simultaneous SO_2/NO_x removal from flue gas generated by burning to simulate the real life event occurring in power plant and other industries. The performance of adsorbents in terms of synthetic method was found to be in the following order: Co_3O_4/adsorbent>IM-Co_3O_4/adsorbent >DP-Co3O4/adsorbent. The Co_3O_4/adsorbent has a high affinity to NO_x adsorption and this influence is associated with the physical and chemical properties of the adsorbent and the operation conditions which were expressed through the plot of the breakthrough curve. The adsorption capacity, breakthrough and saturation times for SO_2 were found to be 1 mg/g, 86 min and 126 min while 130.2 mg/g, 124 min and 160 min were obtained for NOx with respect to the best performed adsorbent. FTIR data provides the confirmation of SO_4^{2-} and NOr accumulation on the adsorbent in the ranges of 700-450 cm−1. Langmuir adsorption model, which is based on constant adsorption energy independence of surface coverage, fitted the experimental res

ISBN: 978-81-932966-1-5

Lampiran